optica

Super-narrow frequency conversion

Roei Remez* and Ady Arie

School of Electrical Engineering, Fleischman Faculty of Engineering, Tel Aviv University, Tel Aviv, Israel
*Corresponding author: roei.remez@gmail.com

Received 4 February 2015; revised 29 March 2015; accepted 16 April 2015 (Doc. ID 233958); published 7 May 2015

The spectral width of a nonlinear converter is usually thought to be inversely proportional to the length of the nonlinear crystal. We present a method to overcome this limitation using the concept of super-oscillations, thus creating an arbitrarily narrow converter. A "super-narrow" frequency doubler was fabricated by appropriate modulation of its quadratic nonlinear coefficient, showing spectral and thermal response that are narrower by 39% and 69% compared to the side lobes and main lobe of the sinc function response of a standard frequency doubling crystal with the same length. This is accompanied by corresponding reduction of the efficiency to 14% and 0.79% with respect to those of the first side lobe and the main lobe. We propose more advanced modulation patterns, and discuss implications such as nonlinear filtering with higher resolution than the standard crystal.

OCIS codes: (140.0140) Lasers and laser optics; (190.0190) Nonlinear optics.

http://dx.doi.org/10.1364/OPTICA.2.000472

What limits the width of a frequency converter? Until now, the limit has been set by the physical length of the converter. For example, in a homogeneous nonlinear crystal of length L, the conversion efficiency as a function of the phase mismatch Δk is proportional to [1] $\mathrm{sinc}^2(\frac{\Delta kL}{2})$, assuming undepleted pump and plane waves. Hence, the width is inversely proportional to the crystal length. This is also the case for quasi-periodic [2,3] and 2D periodic structures [4,5]. There are methods to broaden the width (for example, chirped [6,7] or random [8] poling), but so far it has never been shown how to make it narrower with respect to the length-limited width. There are some applications that require narrow widths, e.g., processing of densely spaced channels in WDM optical communication systems [9,10], isolating a single fluorescent line or a Raman-scattered line [11] in spectroscopy, and generating entangled photons by spontaneous parametric downconversion for quantum information applications in a well-defined frequency [12]. The only available solution to date was provided by increasing the crystal's length. However, this solution is not scalable, consumes a large physical size, and is limited by the available length of crystals (a few centimeters at most). In this Letter we show for the first time, to the best of our knowledge, how to overcome these limitations, and obtain frequency converters with arbitrarily narrow width, by bringing the recently introduced concept of super-oscillations into the nonlinear optics regime.

Super-oscillation refers to the phenomenon of a band-limited function that oscillates faster than its highest Fourier component [13,14]. Super-oscillating functions were used earlier to create super-narrow antennas [15] as well as to focus free-space beams [16,17] or plasmonic beams [18] to a subdiffraction central lobe. Using a super-oscillating lens, it is possible to construct an optical microscope that has subdiffraction resolution of $\lambda/6$ [19], and to create "nondiffracting" super-oscillatory beams [20]. Super-oscillations were also studied in the time domain, enabling time-dependent subdiffraction focusing [21], as well as "super-transmission" through absorbing medium [22]. Here we show that using the same concept of super-oscillation, we can realize a nonlinear frequency converter with arbitrarily narrow frequency response, thus defying the limitation that was thought to be imposed by the Fourier transform relation between the interaction length and the phase-mismatch spectral response.

Under the undepleted pump and plane wave approximation, the amplitude of the generated second harmonic is given by [1]

$$A_2(\Delta k) = \kappa d_{33} \int_{-\infty}^{\infty} \mathrm{d}(z) e^{j\Delta kz} \mathrm{d}z, \quad (1)$$

where $\kappa = i\omega_2 A^2/n_2 c$ is the coupling coefficient (ω_2 and n_2 are the angular frequency and refractive index of the second harmonic, A is the pump amplitude, and c is the speed of light), z is the propagation axis, d_{33} is the nonlinear coefficient, and $d(z)$ is the modulation function of the nonlinear coefficient. Assuming that we have a crystal of length L, we can write the modulation function as $d(z) = f(z) \times \mathrm{rect}(\frac{z}{L})$, where $f(z)$ is an arbitrary function. The second harmonic field is then given by $A_2(\Delta k) = \kappa L \cdot F(\Delta k) \otimes \mathrm{sinc}(\frac{L\Delta k}{2\pi})$, where $\mathrm{sinc}(x) = \frac{\sin(\pi x)}{\pi x}$ and $F(\Delta k)$ is the Fourier transform of $f(z)$. It appears that if one wishes to have a frequency converter with a narrow bandwidth, the best choice is the homogenous case $f(z) = 1$ or equivalently $F(\Delta k) = \delta(\Delta k)$, since any other function for F will result in a wider response once the convolution with the sinc function takes place. In this case, $d(z) = \mathrm{rect}(\frac{z}{L})$; hence $A_2(\Delta k) = d_{33}\kappa L\,\mathrm{sinc}(\frac{L\Delta k}{2\pi})$. This function consists of a central lobe of width $\frac{4\pi}{L}$, and a series of side lobes of width $\frac{2\pi}{L}$. Another commonly used option is to periodically modulate the nonlinear coefficient, in order to achieve quasi-phase-matched interaction. In this case, $f(z) = \text{sign}(\cos(\Delta k_0 z))$, and therefore $A_2 = d_{33}\kappa L \sum_{m=-\infty}^{\infty} \frac{2}{\pi m} \text{sinc}(L \frac{\Delta k - m\Delta k_0}{2\pi})$. Here the sum is over the odd m values only. This function is essentially an infinite series of sinc functions, but for a given process we are usually interested in a small region near one particular spatial frequency that quasi-phase matches the interaction (which had initial mismatch of Δk_0). In this region, the spectral response has the same characteristics as the homogenous crystal, i.e., a central lobe of width $\frac{4\pi}{L}$ and side lobes of width $\frac{2\pi}{L}$. The same width is also obtained in quasi-periodic [2] and 2D photonic crystals [4].

We now wish to design a crystal with a central lobe that is as small as we wish. As we showed in Eq. (1), there is a Fourier transform relation between the nonlinearity as a function of interaction length and the second harmonic signal (or conversion efficiency) as a function of phase mismatch. We therefore look for a super-oscillating function in Δk coordinates, which remains band-limited in its Fourier transformed (i.e., crystal) coordinates to a fixed interaction length. Specifically, we aim for efficiency with response of

$$I_2(\Delta k) \propto \left(\cos \frac{L_1 \Delta k}{2} - s\right)^2, \tag{2}$$

where $0 < s < 1$ defines the offset of the cosine function [see Fig. 1(a)]. This function has a central lobe of width $\frac{4}{L_1}\cos^{-1} s$. It exhibits super-oscillation around $\Delta k = 0$, since as s approaches 1 and L_1 remains constant, the central lobe gets smaller, but the maximum Fourier frequency remains L_1 and is independent of the width of the oscillation.

In order to realize a super-narrow frequency converter, the quadratic nonlinear coefficient should be spatially modulated. In ferroelectric crystals this can be done by electric field poling [23,24], and in this case the modulation is binary, i.e., $f(z)$ can be either 1 or −1. We design $d(z)$ using methods that were previously developed in binary computer-generated holography [25]:

$$d(z) = \text{sign}(\cos(\Delta k_0 z + \phi(z)) - \cos(\pi q(z))), \tag{3}$$

where $\phi(z)$ and $q(z)$ are arbitrary functions that determine the converter's phase and amplitude response, respectively, and $-\frac{L}{2} < z < \frac{L}{2}$. The amplitude is then written as an infinite sum, for which the first order (around Δk_0) is

$$A_2^{(1)}(\Delta k) = \frac{2\kappa d_{33}}{\pi} \int_{-\frac{L}{2}}^{\frac{L}{2}} \sin(\pi q(z)) e^{j\phi(z)} e^{j(\Delta k + \Delta k_0)z} \text{d}z. \tag{4}$$

To achieve the response described in Eq. (2), we aim for the second harmonic amplitude around Δk_0 to be proportional to the square root of the intensity $I_2(\Delta k)$, i.e.,

$$g(\Delta k) \equiv \cos \frac{L_1 \Delta k}{2} - s, \tag{5}$$

where $L_1 < L$ and s are constants. A naïve approach would suggest to choose functions $\phi(z)$ and $q(z)$ such that the expression $\sin(\pi q(z)) e^{j\phi(z)}$ would be equal to the Fourier transform of $g(\Delta k)$. However, $\text{FT}\{g(\Delta k)\}$ contains three delta functions, as shown in Fig. 1(b); hence this modulation pattern cannot be fabricated in a real nonlinear crystal. However, we can broaden these delta functions by convolving them with a rect function of width Z_0, so that the nonlinear modulation would be possible by electric field poling of ferroelectrics, as illustrated in Figs. 1(c) and 1(d). We then choose $\phi(z)$ and $q(z)$ according to the following equation:

$$\sin(\pi q(z)) e^{j\phi(z)} \equiv \frac{\text{IFT}\{g(\Delta k)\} \circledast \text{rect}\left(\frac{z}{Z_0}\right)}{\max\left[\left|\text{IFT}\{g(\Delta k)\} \circledast \text{rect}\left(\frac{z}{Z_0}\right)\right|\right]}, \tag{6}$$

where $Z_0 = L - L_1$. Solving for $q(z)$ and $\phi(z)$ and substituting in Eq. (3), we obtain

$$d(z) = \begin{cases} \text{sign}\left(\cos(\Delta k_0 z + \pi) - \sqrt{1 - \left(\frac{s}{\max(s, 0.5)}\right)^2}\right) & |Z| < \frac{Z_0}{2} \\ \text{sign}\left(\cos(\Delta k_0 z) - \sqrt{1 - \left(\frac{1}{2\max(s, 0.5)}\right)^2}\right) & \frac{L_1 - Z_0}{2} < |Z| < \frac{L}{2} \end{cases}. \tag{7}$$

The upper row describes the modulation pattern in the middle section of the crystal, and the bottom row describes the modulation pattern near the two edges of the crystal. There is a constant duty cycle and phase in each one of these three sections. The central section has a π phase and a different duty cycle with respect to the two peripheral sections. When we choose $L_1 = \frac{2}{3}L$ these three separate sections cover the entire length of the crystal.

The amplitude around Δk_0 will therefore be

$$A_2^{(1)}(\Delta k) = \frac{2Z_0 \kappa d_{33}}{\max(s, 0.5)\pi} g(\Delta k - \Delta k_0) \times \text{sinc}\left(\frac{Z_0}{2\pi}[\Delta k - \Delta k_0]\right). \tag{8}$$

The efficiency is proportional to the square of the amplitude, hence to $g^2(\Delta k - \Delta k_0)\text{sinc}^2(\frac{Z_0}{2\pi}[\Delta k - \Delta k_0])$, and therefore the power of the second harmonic is equal to zero for $\Delta k - \Delta k_0 = \pm\frac{2}{L_1}\cos^{-1} s$. The multiplication with the sinc function does not

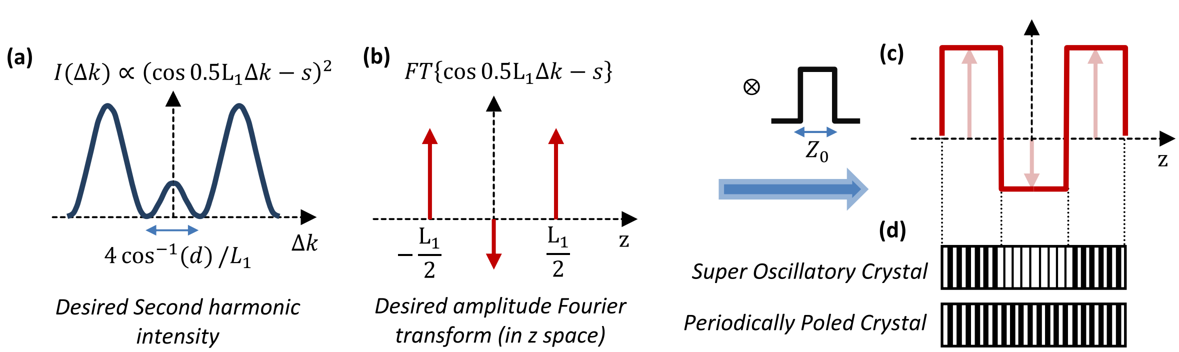

Fig. 1. Design process. (a) Desired intensity profile, (b) desired amplitude Fourier transform, (c) designed amplitude Fourier transform after convolution with rect function, and finally (d) resulting poling design in comparison with a standard periodically poled crystal.

change the central lobe width (the super-oscillation) in $g^2(\Delta k - \Delta k_0)$, since the central lobe of the sinc is wider than that of the super-oscillatory function. As s approaches 1, the width of the converter's central lobe, $\frac{4}{L_1}\cos^{-1} s$, gets smaller and smaller. That is, by increasing s one can achieve an arbitrarily small width, using crystal of size L, unconstrained to s. This is not without penalty, since the power of the generated wavelength is decreasing as $(1/s - 1)^2$ at $\Delta k = \Delta k_0$ (the center of the oscillation). Figures 2(a) and 2(c) show the simulated normalized efficiency, as a function of pump wavelength and crystal temperature, for a 10 mm periodically poled $KTiOPO_4$ crystal for doubling 1550 nm radiation and for a super-narrow design, with $s = 0.68$ and $Z_0 = 3.3$ mm. This converter's central lobe width is 26% smaller than the side lobes of the periodically poled sinc function, and 58% smaller than the sinc main lobe. This narrow response enables high-resolution nonlinear filtering, for example, in sum-frequency processes, as we will discuss later.

In order to test this concept, we designed and fabricated a crystal with the modulation pattern described by Eq. (7) and measured its spectral and thermal bandwidths. The crystal was designed for doubling 1550 nm pump light based on an e-ee process (both the pump and SH are polarized along the crystal's Z direction), at a temperature of 100°C. A 10-mm-long, 1-mm-thick KTP crystal was electric field poled according to the super-narrow design algorithm, with parameters $s = 0.68$ and $Z_0 = 3.3$ mm, resulting in three sections of identical 3.3 mm length and with a central poling period of 24.7 μm. The central section had a duty cycle of 0.5, whereas the two outer sections had a duty cycle of 0.26. For comparison, a parallel channel of the same crystal was periodically poled with a period of 24.7 μm and a duty cycle of 0.5. Each one of the two channels had a width of 1 mm. The pump beam was generated by a tunable diode laser, followed by an erbium-doped fiber amplifier and a fiber polarization controller. It was modulated using a chopper and focused to a waist of 62 μm in the middle of the crystal. The

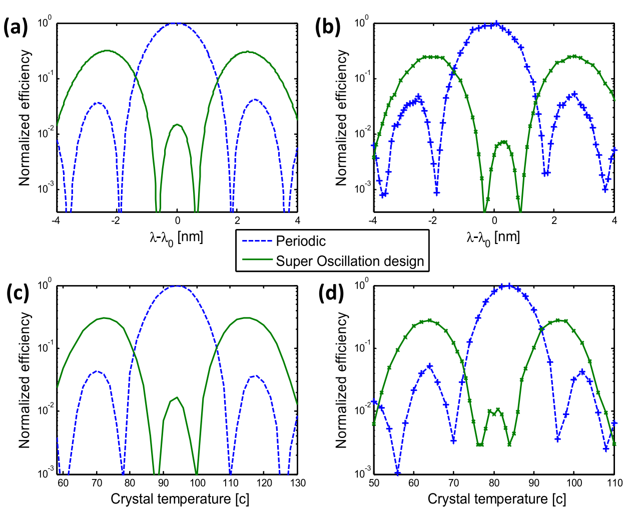

Fig. 2. Normalized efficiency. (a) Simulated conversion efficiency of a Gaussian pump beam in a 10 mm KTP crystal with a super-oscillation design (in solid green), in comparison with periodically poled crystal (dashed blue), for both a waist of 62 μm and $\lambda_0 = 1550$ nm. (b) Experimental results for the same parameters. (c) Simulation and (d) measurements of normalized efficiency versus crystal temperature, at wavelength of 1555 nm. All graphs are normalized to the peak efficiency of the sinc response of the periodically poled crystal.

crystal was held on a temperature-controlled mount. The second harmonic power was measured using a silicon detector connected to a lock-in amplifier.

Figure 2(b) presents the measured conversion efficiency versus the pump wavelength at a fixed crystal temperature of 50°C. This temperature was different from the design temperature of 100°C, probably owing to the limited accuracy of the Sellmeier equations that we used in the design process [26] (a different Sellmeier equation [27] gave a poorer match). A spectral bandwidth of 1.1 nm is observed, 39% smaller than the 1.8 nm width of the sinc side lobes in the reference periodically poled channel. The super-oscillation peak is also 69% narrower than the 3.6 nm width of the sinc's central lobe.

The difference between the measured width (1.1 nm) and the theoretical calculation (1.4 nm) can be explained by systematic error in domain width; for example, if each domain in the crystal with positive sign of the nonlinear coefficient were wider by 1 μm with respect to the design (e.g., duty cycle of 0.54 (0.3) instead of 0.5 (0.26) in the central (outer) region of the crystal), this would effectively increase the value of s in Eq. (5) with respect to the cosine amplitude, thereby leading to a narrower bandwidth that is consistent with our measurements.

The narrow response can also be seen as a function of the crystal's temperature, which changes the phase-matching conditions owing to the thermal dispersion of the crystal. Simulation and experimental results of the temperature dependence for both periodically poled and super-oscillatory crystal are presented in Figs. 2(c) and 2(d). The measured temperature width of the super-oscillating channel was 7°C, compared with the sinc side lobe (central lobe) width of 12° (24°) in the periodically poled channel. This is compared with simulation values of 12° for the super-oscillation and 16° for the periodically poled side lobe. The differences between the simulation and measurements can be due to inaccuracies in the Sellmeier equation, and they are observed in both the periodically poled and the super-oscillating cases. However, the same ratio of super-oscillation to sinc side lobe width remained between the measurements versus wavelength and versus temperature, which indicates that the super-oscillation exists in the same way over temperature. We note that the thermal dispersion measurements were performed at a slightly higher pump wavelength of 1555 nm, in order to shift the central temperature point to 80°C, thereby enabling easier characterization of the thermal response with our experimental setup.

By measuring the second harmonic power as a function of the pump power we derived a conversion efficiency of 3.4×10^{-4}% per W for the super-oscillation crystal at the optimal wavelength of 1550.8 nm. For comparison, the peak efficiency of the periodically poled reference channel was 4.3×10^{-2}% per W, and the first side lobe efficiency is 2.5×10^{-3}% per W. The theoretical conversion efficiencies are 2.4×10^{-3}% per W, 0.17% per W, and 6.1×10^{-3}% per W, respectively. The experimental efficiency of the super-oscillation peak is therefore decreased by a factor of 0.0079 compared to the sinc main lobe's peak and 0.14 compared to the first side lobe peak. The 1 μm domain broadening error that we mentioned before can also explain the difference in the ratio (of the super-oscillation peak to the sinc peak) between the experimental and theoretical predictions.

In the designs so far, the efficiency is rapidly increasing beyond the super-oscillation region. This could generate a problem when the desired signal to be filtered is not very narrow, which raises the

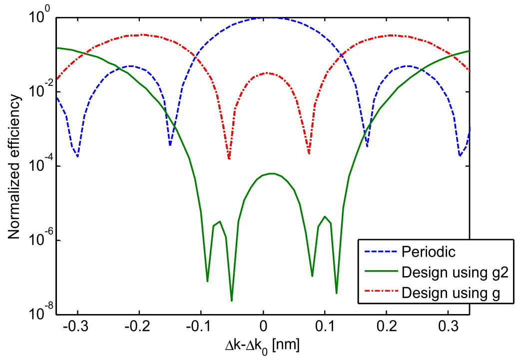

Fig. 3. Simulation for isolated super-narrow peak design using function from Eq. (9) (solid green) with $L = 40$ mm, $Z_0 = 8$ mm, $s_1 = 0.8$, $s_2 = 0.08$, for KTP and 1550 nm pump; compared with the periodic design of a crystal of the same length (dashed blue); and design using g function of Eq. (5) (point-dashed red) with $L = 40$ mm, $Z_0 = 13.3$, $s = 0.68$.

need to push these side lobes away from the super-oscillation area. This can be done, for example, by using prolate spherical wave functions (PSWFs) [28,29]. We present here a different approach to this problem. Instead of the function in Eq. (5) we can use the following function:

$$g_2(\Delta k) \equiv \left(\cos\frac{L_1\Delta k}{4} - s_1\right)^2 - s_2, \qquad \textbf{(9)}$$

where $0 \le s_1, s_2 \le 1$. Using the exact same method, the efficiency will be proportional to $g_2^2(\Delta k - \Delta k_0)\mathrm{sinc}^2(\frac{Z_0}{2\pi}[\Delta k - \Delta k_0])$. Roughly, s_1 controls the central lobe width, and s_2 controls the height and the width of the first side lobes. Figure 3 shows the resulting normalized efficiency. The same process can be repeated to push the side lobes even further, by using a higher order of the function series, $g_3(\Delta k) \equiv ((\cos\frac{L_1\Delta k}{8} - s_1)^2 - s_2)^2 - s_3$; however, each order results in a rapid decrease of the peak of the oscillation.

In this Letter, we have demonstrated a new method for creating an arbitrarily narrow frequency converter, which, unlike the conventional nonlinear crystals, is no longer determined by the crystal's length. We implemented this concept experimentally by modulating the nonlinear coefficient of a KTP crystal using the electric field poling method and demonstrated super-oscillation in the converter frequency response—as a function of the pump wavelength and as a function of the crystal's temperature. While here we utilized the concept of super-oscillation to design a frequency doubler with an isolated peak in the frequency conversion spectrum, the method can be further extended using different super-oscillating functions [28,30].

In this work we demonstrated narrow bandwidth in second harmonic generation, but the same method can be readily used for other types of quadratic nonlinear interactions such as sum- and difference-frequency generation. An interesting possibility is sum-frequency generation of two nearby pump wavelengths. In a regular crystal, the sum-frequency signal is created together with two unwanted second harmonic signals from each of the two inputs. However, we can filter out these second harmonic signals by placing the two pump wavelengths at the zero-efficiency nodes of the efficiency curve. A super-oscillation crystal enables us to achieve this result in a crystal that is much shorter with respect to a regular crystal. Another interesting extension is to improve the efficiency of the super-oscillating converter by using high pump power. The SO converter can provide conversion efficiency of 7% with relatively modest peak power of 3 kW, but at higher pump power the undepleted pump approximation [Eq. (1)] no longer holds and the spectral shape is distorted. We believe that this work opens exciting new possibilities for nonlinear processing and nonlinear filtering of optical signals in optical communications, spectroscopy, and quantum information applications. Moreover, this concept can be extended to other types of nonlinear interactions that require phase matching, e.g., nondegenerate four-wave mixing, as well as to linear systems that require coupling between waves that have different wavevectors, for example, coupling between a free-space beam and either a waveguide mode or a surface plasmon polariton wave.

Israel Science Foundation (1310/13); The German-Israeli Project cooperation (DIP).

REFERENCES

1. R. W. Boyd, *Nonlinear Optics*, 3rd ed. (Academic, 2008).
2. R. Lifshitz, A. Arie, and A. Bahabad, Phys. Rev. Lett. **95**, 133901 (2005).
3. S. Zhu, Y. Zhu, and N. Ming, Science **278**, 843 (1997).
4. A. Arie, N. Habshoosh, and A. Bahabad, Opt. Quantum Electron. **39**, 361 (2007).
5. V. Berger, Phys. Rev. Lett. **81**, 4136 (1998).
6. M. Nasr, S. Carrasco, B. Saleh, A. Sergienko, M. Teich, J. Torres, L. Torner, D. Hum, and M. Fejer, Phys. Rev. Lett. **100**, 183601 (2008).
7. H. Suchowski, D. Oron, A. Arie, and Y. Silberberg, Phys. Rev. A **78**, 063821 (2008).
8. I. Varon, G. Porat, and A. Arie, Opt. Lett. **36**, 3978 (2011).
9. M. Kim, J. Ahn, J. Kim, J. Ju, and M. Lee, ETRI J. **27**, 312 (2005).
10. C. Langrock, S. Kumar, J. E. McGeehan, A. E. Willner, and M. M. Fejer, J. Lightwave Technol. **24**, 2579 (2006).
11. I. Galli, S. Bartalini, S. Borri, P. Cancio, D. Mazzotti, P. De Natale, and G. Giusfredi, Phys. Rev. Lett. **107**, 270802 (2011).
12. P. Ben Dixon, J. H. Shapiro, and F. N. C. Wong, Opt. Express **21**, 5879 (2013).
13. M. Berry, *Quantum Coherence and Reality, Celebration of the 60th Birthday of Yakir Aharonov*, J. S. Anandan and J. L. Safko, eds. (World Scientific, 1994), pp. 55–65.
14. Y. Aharonov, J. Anandan, S. Popescu, and L. Vaidman, Phys. Rev. Lett. **64**, 2965 (1990).
15. P. Woodward and J. Lawson, J. Inst. Electr. Eng. Part 3 **95**, 363 (1948).
16. G. Di Francia, Nuovo Cimento **9**, 426 (1952).
17. E. T. F. Rogers and N. I. Zheludev, J. Opt. **15**, 094008 (2013).
18. G. Yuan, E. T. F. Rogers, T. Roy, L. Du, Z. Shen, and N. I. Zheludev, *CLEO: QELS_Fundamental Science* (Optical Society of America, 2014).
19. E. T. F. Rogers, J. Lindberg, T. Roy, S. Savo, J. E. Chad, M. R. Dennis, and N. I. Zheludev, Nat. Mater. **11**, 432 (2012).
20. E. Greenfield, R. Schley, I. Hurwitz, J. Nemirovsky, K. G. Makris, and M. Segev, Opt. Express **21**, 13425 (2013).
21. M. Dubois, E. Bossy, S. Enoch, S. Guenneau, G. Lerosey, and P. Sebbah, Phys. Rev. Lett. **114**, 013902 (2015).
22. Y. Eliezer and A. Bahabad, Opt. Express **22**, 31212 (2014).
23. A. Arie and N. Voloch, Laser Photon. Rev. **4**, 355 (2010).
24. M. Yamada, N. Nada, M. Saitoh, and K. Watanabe, Appl. Phys. Lett. **62**, 435 (1993).
25. W. H. Lee, Appl. Opt. **18**, 3661 (1979).
26. K. Kato and N. Umemura, Appl. Opt. **41**, 5040 (2002).
27. S. Emanueli and A. Arie, Appl. Opt. **42**, 6661 (2003).
28. F. M. Huang and N. I. Zheludev, Nano Lett. **9**, 1249 (2009).
29. D. Slepian and H. Pollak, Bell Syst. Tech. J. **40**, 43 (1961).
30. M. V. Berry and S. Popescu, J. Phys. A **39**, 6965 (2006).